Trends in Computational and Applied Mathematics, **23**, N. 3 (2022), 499-513
Sociedade Brasileira de Matemática Aplicada e Computacional
Online version ISSN 2676-0029
www.scielo.br/tcam
doi: 10.5540/tcam.2022.023.03.00499

Health Professionals and the Dynamics of COVID-19 in Manaus during the First Wave

R. C. BASSANEZI[1], L. T. TAKAHASHI[2], A. L. O. SOARES[3], M. H. R. LUIZ[4*], S. D. DE SOUZA[5] and D. F. GOMES[6]

Received on August 11, 2021 / Accepted on February 16, 2022

ABSTRACT. A model is made for the dynamics of the transmission of the new SARS-CoV-2 coronavirus, which caused the COVID-19 pandemic. This model is based on the Susceptible–Infectious–Recovered model with heterogeneity in the susceptible population and in the infectious population. The susceptible population is divided into two subpopulations: individuals who are health professionals and individuals who are not. The infectious population is also divided into two subpopulations: individuals who are hospitalized and individuals who are not. A qualitative analysis of the theoretical model is performed, as well as simulations with official data regarding COVID-19 in the city of Manaus, Amazonas, Brazil, which corroborate the profile of the solution curves defined by the model.

Keywords: population heterogeneity, Lyapunov function, basic reproduction number.

1 INTRODUCTION

In December 2019, several cases of pneumonia occurred in Wuhan, China, caused by a new coronavirus, named SARS-CoV-2 by the International Coronavirus Study Committee [6]. This new coronavirus is the causative agent of the COVID-19 disease, which, on March 11, 2020, was declared a pandemic by the World Health Organization (WHO). The most common symptoms

*Corresponding author: Monica Helena Ribeiro Luiz – E-mail: monicahrl@ifsp.edu.br
[1]Departamento de Matemática Aplicada, IMECC, Universidade Estadual de Campinas, R. Sérgio Buarque de Holanda, 651, 13083-859, Campinas, SP, Brazil – E-mail: rodney@ime.unicamp.br https://orcid.org/0000-0002-5219-5319
[2]Departamento de Matemática, ICE, Universidade Federal de Juiz de Fora, R. José Lourenço Kelmer, s/n, 36036-900, Juiz de Fora, MG, Brazil – E-mail: ltiemi@gmail.com https://orcid.org/0000-0002-8918-3899
[3]Departamento de Matemática, ICET, Universidade Federal de Mato Grosso, Av. Fernando Corrêa da Costa, 2367, 78060-900, Cuiabá, MT, Brazil – E-mail: ligiaoenning@hotmail.com https://orcid.org/0000-0002-6076-2037
[4]Departamento de Ciências e Matemática, Instituto Federal de São Paulo, R. Pedro Vicente, 625, 01109-010, São Paulo, SP, Brazil – E-mail: monicahrl@ifsp.edu.br https://orcid.org/0000-0001-9189-7615
[5]Departamento de Matemática, Universidade Federal do Amazonas, Av. General Rodrigo Octavio Jordão Ramos, 1200, 69067-005, Manaus, AM, Brazil – E-mail: silviasouza@ufam.edu.br https://orcid.org/0000-0002-6862-7307
[6]Departamento de Ensino, Instituto Federal do Maranhão, Rodovia BR-226, Km 303, s/n, 65950-000, Barra do Corda, MA, Brazil – E-mail: diego.gomes@ifma.edu.br https://orcid.org/0000-0002-7727-1090

caused by SARS-COV-2 are fever, tiredness and a dry cough. In addition, some people have reported pain, nasal congestion, headache, conjunctivitis, sore throat, diarrhea, loss of taste or smell, and rash or discoloration of fingers or toes [12].

One year after the start of the pandemic, by March 22, 2021, more than 123.5 million cases and more than 2.7 million deaths due to Covid-19 were confirmed worldwide [12]. The first confirmed case of COVID-19 in Brazil, according to the Ministry of Health, occurred on February 26, 2020, and by March 22, 2020 there were more than 11.9 million confirmed cases and 294,115 deaths due to COVID-19 in the world [9, 12]. The first wave in Brazil had its peak between the months of July to September 2020, and in November 2020 the number of cases started to grow again, characterizing the beginning of the second wave. Also in September, when the national scenario was stabilizing with 4.7 million confirmed cases and 141,741 deaths [18], there was an increase in the number of cases in the city of Manaus, the capital of the state of Amazonas, characterizing and starting the second pandemic wave in that city.

Manaus had its first confirmed case of COVID-19 on March 11, 2020, after twelve suspected cases and eight discarded, and was, in April and May, the first Brazilian capital to suffer a health system collapse. After the collapse, with the reduction of cases, social isolation eased in June, which probably led to the increase in cases in September. Understanding how Covid-19's dynamics occurred in the city of Manaus is fundamental to finding ways to contain it in that region.

There are several articles that mathematically portray the dynamics of COVID-19 transmission based on the classic model of the Susceptible–Infectious–Recovered (SIR) type which was developed by Kermack and McKendrick in 1927 [8] (see [2], [5], [11], [13], [10]), which assumes that the susceptibility and the infectivity for the population are homogeneous.

In other words, any susceptible individual has the same probability of becoming infected through encountering an infectious individual; moreover, infectious individuals have the same probability of transmitting the disease. However, health professionals are more susceptible to contracting this disease because they are in direct contact with patients, moreover, each infectious individual responds differently, and may present mild to moderate symptoms (not requiring hospitalization) or severe symptoms (requiring hospitalization).

This paper proposes a model in which a specific dynamic is considered for susceptible individuals who are health professionals, different from the dynamics for individuals who are not health professionals. Two distinct classes of infectious persons are also considered, according to the severity of the disease: requiring hospitalization or not, and it is found that these characteristics directly influence the transmission dynamics of COVID-19.

A qualitative analysis of the stability of the theoretical model is carried out [1, 3], in which the Basic Reproduction Number, $\mathscr{R}_0$, is obtained by the Next Generation Matrix method [17]. In addition, simulations of the model are carried out, which are then compared with data released by the city of Manaus, Amazonas, Brazil, in the period from March 31 to September 1, 2020, when the first wave of COVID-19 occurred.

2 MATHEMATICAL MODEL

In this section, a compartmental epidemiological model is presented for a preliminary analysis of the dynamics of COVID-19. It is assumed that part of the population is in quarantine, but the model does not consider a specific compartment for that part of the population. Quarantine is reflected in the parameters β_i, $i = 1,2$ that indicate the strength of infection, which are obtained empirically. It is noteworthy that the period of validity of the model is short, as it is assumed that individuals do not change their behaviour, that is, individuals who are in quarantine do not leave quarantine, and that individuals who are not in quarantine remain so. Thus, the proposed model is idealized, and not realistic, as it is intrinsic to human beings to change their behaviour and not have specific periods for them to occur. The population size N must be the total population minus the quarantined, which remains constant during the first wave, and large enough to consider its classes as continuous variables with respect to the time variable t, scaled in days. With respect to time, the 6 disjoint classes (subpopulations) considered are denoted by the variables $S_1(t)$, $S_2(t)$, $I_1(t)$, $I_2(t)$, $C(t)$ and $D(t)$, and defined as:

- $S_1(t)$ is the number of susceptible individuals who are not health professionals;
- $S_2(t)$ is the number of susceptible individuals who are healthcare professionals;
- $I_1(t)$ is the number of infectious individuals who are asymptomatic or symptomatic with only mild to moderate symptoms who are not hospitalized;
- $I_2(t)$ is the number of symptomatic infectious individuals who require hospitalization;
- $C(t)$ is the number of individuals recovering from COVID-19;
- $D(t)$ is the number of individuals who die due to COVID-19.

Therefore, at time t, the total population is given by

$$N = S_1(t) + S_2(t) + I_1(t) + I_2(t) + C(t) + D(t). \tag{2.1}$$

In Figure 1, the compartmental model based on the observed dynamics for COVID-19 is presented, considering these six classes of the population interacting knowing that the disease is favoured by a larger number of contacts between the susceptible and infectious, as in all direct transmission diseases.

It is assumed that health professionals who are in "direct contact" with infectious patients, in general, have a greater degree of susceptibility than any other individual and infections occur in the hospital environment. Thus, susceptible individuals were compartmentalized into two classes, S_1 and S_2. It is also assumed that health professionals become infected after a successful encounter with hospitalized infectious individuals, $\beta_2 S_2 I_2$, and other individuals who are in S_1 can be infected after a successful encounter with infectious individuals not hospitalized, $\beta_1 S_1 I_1$. All newly infected people migrate to class I_1, but a part of them, λI_1, develop severe symptoms, requiring

hospitalization, and thus migrate to class I_2. The terms $\gamma_1 I_1$ and $\gamma_2 I_2$ represent individuals who have recovered from COVID-19 and therefore migrate from their classes to class C. It is also assumed that, due to their health status, only individuals in I_2 may die, which is represented by the term $-\mu I_2$ in the class I_2 and, therefore, μI_2 represents entry into class D. Note that this model does not consider vital dynamics, and so the deaths are exclusively due to COVID-19. Note also that the parameters β_1, β_2, γ_1, γ_2, λ and μ are positive constants that depend exclusively on the characteristics of COVID-19 in the population.

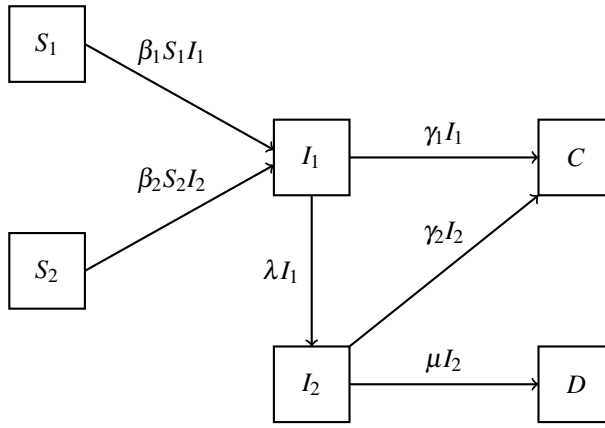

Figure 1: Compartmental model for the dynamics of COVID-19 transmission, considering two classes for the susceptible population: health professionals, S_2, and those who are not health professionals, S_1; two classes of infectious divided according to symptoms: mild to moderate, I_1, and severe, I_2. In addition there is the class of cured individuals, C, and another class, the dead, D. Made by the authors.

Thus, for the study of the dynamics of COVID-19 transmission, the following system of ordinary differential equations is considered:

$$\begin{aligned} S_1' &= -\beta_1 S_1 I_1 \\ S_2' &= -\beta_2 S_2 I_2 \\ I_1' &= \beta_1 S_1 I_1 + \beta_2 S_2 I_2 - \gamma_1 I_1 - \lambda I_1 \\ I_2' &= \lambda I_1 - \gamma_2 I_2 - \mu I_2 \\ C' &= \gamma_1 I_1 + \gamma_2 I_2 \\ D' &= \mu I_2, \end{aligned} \tag{2.2}$$

where ($'$) represents the differentiation with respect to t: $\frac{d}{dt}$.

3 QUALITATIVE ANALYSIS

Once $S_1(t)$, $S_2(t)$, $I_1(t)$ and $I_2(t)$ are known, it is possible to obtain $C(t)+D(t)$ by equation (2.1) for each instant of time t since N is constant; in addition, C and M do not interfere in the dynamics of the other subpopulations, so for the qualitative analysis of the models, the last two equations of system (2.2) are disregarded. Moreover, the system of equations (2.2) is reordered to fit the theory involving the Next Generation Matrix presented in [17], considering then the new system

$$\begin{aligned} I_1' &= \beta_1 S_1 I_1 + \beta_2 S_2 I_2 - \gamma_1 I_1 - \lambda I_1 \\ I_2' &= \lambda I_1 - \gamma_2 I_2 - \mu I_2 \\ S_1' &= -\beta_1 S_1 I_1 \\ S_2' &= -\beta_2 S_2 I_2. \end{aligned} \tag{3.1}$$

The system (3.1) can now be rewritten as

$$\mathbf{x}' = f(\mathbf{x}), \tag{3.2}$$

where $\mathbf{x} = \big(I_1, I_2, S_1, S_2\big)$ is the state variable and $f : \mathbb{R}^4 \to \mathbb{R}^4$ is a function with $f = (f_1, f_2, f_3, f_4)$ coordinates given by

$$I_1' = f_1(\mathbf{x}),\ \ I_2' = f_2(\mathbf{x}),\ \ S_1' = f_3(\mathbf{x}) \ \text{ and } \ S_2' = f_4(\mathbf{x}).$$

Note that f is of class C^∞ and, therefore, the (3.1) system has a single solution for each initial condition $\mathbf{x}_0 \in \mathbb{R}^4$. Consider the set

$$\Omega = \big\{(I_1, I_2, S_1, S_2) \in \mathbb{R}^4_+ \,|\, I_1 + I_2 + S_1 + S_2 \leq N\big\}$$

as the biological space, that is, the epidemiologically feasible space.

3.1 Equilibrium Points

The system (3.1) in four-dimensional phase space (I_1, I_2, S_1, S_2) has infinitely many points of equilibrium, making up the set given by

$$\Omega^* = \big\{(0, 0, S_1, S_2) \in \mathbb{R}^4_+ \,|\, S_1 + S_2 \leq N\big\}, \tag{3.3}$$

and the system (3.1) does not admit non-trivial equilibrium points.

Theorem 3.1. *The biological space Ω of the model* (3.1) *is positively flow-invariant.*

Proof. It needs to be shown that the solution curve from an initial condition in Ω does not cross the boundary $\partial\Omega$, for Ω to $t > 0$. Note that $\partial\Omega$ is composed of 5 subspaces, which are denoted by Ω_i, $i = 1, \ldots, 5$, that is,

$$\partial\Omega = \Omega_1 \cup \Omega_2 \cup \Omega_3 \cup \Omega_4 \cup \Omega_5.$$

Therefore, it will be proved that the field f associated with system (3.2) defined on Ω_i, $i = 1,2,5$, points to within Ω and that Ω_i, $i = 3,4$, are invariant. Writing e_i, $i = 1,\ldots,4$ for the vectors of the canonical basis of $\mathbb{R}^4$, we have that:

1. If $q \in \Omega_1 \backslash \Omega^*$, with $\Omega_1 = \left\{(I_1,I_2,S_1,S_2) \in \mathbb{R}^4_+ | I_1 = 0, I_2 + S_1 + S_2 \leq N\right\}$, then $f(q)$ points into Ω. In fact, $\left\langle f(q), e_1 \right\rangle = \beta_2 S_2 I_2 \geq 0$. Furthermore,

   (a) if $S_1 = 0$, then $\left\langle f(q), e_3 \right\rangle = 0$ and if $S_1 = 0$ and $I_2 + S_2 = N$, then $\left\langle f(q), e_2 + e_4 \right\rangle = -(\gamma_2 + \mu)I_2 - \beta_2 S_2 I_2 < 0$;

   (b) if $S_2 = 0$, then $\left\langle f(q), e_4 \right\rangle = 0$. Moreover, if $I_2 + S_1 = N$, then $\left\langle f(q), e_2 + e_3 \right\rangle = -(\gamma_2 + \mu)I_2 < 0$;

   (c) if $S_1 \neq 0$, $S_2 \neq 0$ and $I_2 + S_1 + S_2 = N$, then $\left\langle f(q), e_2 + e_3 + e_4 \right\rangle = -(\gamma_2 + \mu)I_2 - \beta_2 S_2 I_2 < 0$, and

   (d) if $I_2 = N$, then $\left\langle f(q), e_2 \right\rangle = -\|f(q)\| < 0$.

2. If $q \in \Omega_2 \backslash \Omega^*$, with $\Omega_2 = \left\{(I_1,I_2,S_1,S_2) \in \mathbb{R}^4_+ | I_2 = 0, I_1 + S_1 + S_2 \leq N\right\}$, then $f(q)$ points into Ω. The proof is analogous to the one for Ω_1.

3. If $q \in \Omega_3 \backslash \Omega^*$, with $\Omega_3 = \left\{(I_1,I_2,S_1,S_2) \in \mathbb{R}^4_+ | S_1 = 0,\ I_1 + I_2 + S_2 \leq N\right\}$, then $f(q)$ points into Ω_3. In fact, in this case, $\left\langle f(q), e_3 \right\rangle = 0$. Furthermore,

   (a) if $I_1 = 0$, then $\left\langle f(q), e_1 \right\rangle = \beta_2 S_2 I_2 \geq 0$. Furthermore, if $S_2 = 0$, then $\left\langle f(q), e_1 \right\rangle = 0$ and $\left\langle f(q), e_2 \right\rangle = -\|f(q)\| < 0$ and if $I_2 + S_2 = N$, then $\left\langle f(q), e_2 + e_4 \right\rangle = -(\gamma_2 + \mu)I_2 - \beta_2 S_2 I_2 < 0$;

   (b) if $I_2 = 0$, then $\left\langle f(q), e_2 \right\rangle = \lambda I_1 > 0$. Furthermore, if $S_2 = 0$, then $\left\langle f(q), e_1 \right\rangle = -(\gamma_1 + \lambda)I_1 < 0$ and $\left\langle f(q), e_4 \right\rangle = 0$, and if $I_1 + S_2 = N$, then $\left\langle f(q), e_1 + e_4 \right\rangle = -(\gamma_1 + \lambda)I_1 < 0$ and $\left\langle f(q), e_1 + e_2 + e_4 \right\rangle = -\gamma_1 I_1 < 0$;

   (c) if $S_2 = 0$, then $\left\langle f(q), e_4 \right\rangle = 0$. Furthermore, if $I_1 + I_2 = N$, then $\left\langle f(q), e_1 + e_2 \right\rangle = -\gamma_1 I_1 - (\gamma_2 + \mu)I_2 < 0$;

   (d) if $I_1 + I_2 + S_2 = N$, then $\left\langle f(q), e_1 + e_2 + e_4 \right\rangle - \gamma_1 I_1 - (\gamma_2 + \mu)I_2 < 0$ and

   (e) if $I_1 = N$, then $\left\langle f(q), e_1 \right\rangle = -(\gamma_1 + \lambda)N < 0$, $\left\langle f(q), e_2 \right\rangle = \lambda N > 0$ and $\left\langle f(q), e_1 + e_2 \right\rangle = -\gamma_1 N < 0$.

4. If $q \in \Omega_4 \setminus \Omega^*$, with $\Omega_4 = \left\{(I_1,I_2,S_1,S_2) \in \mathbb{R}^4_+ | S_2 = 0, I_1 + I_2 + S_1 \leq N\right\}$, then $f(q)$ points into Ω_4. The proof is analogous to the one for Ω_3.

5. If $q \in \Omega_5 \setminus \Omega^*$, with $\Omega_5 = \left\{(I_1,I_2,S_1,S_2) \in \mathbb{R}^4_+ | I_1 + I_2 + S_1 + S_2 = N\right\}$, then $f(q)$ points into Ω. In fact, in this case $\left\langle f(q), \eta \right\rangle = -\gamma_1 I_1 - (\gamma_2 + \mu)I_2 < 0$, with $\eta = e_1 + e_2 + e_3 + e_4$. Furthermore, if $I_1 = 0$, then $\left\langle f(q), e_1 \right\rangle = \beta_2 S_2 I_2 \geq 0$. Furthermore,

(a) if $S_1 = 0$, then

i. if $I_2 + S_2 = N$, then $\langle f(q), e_2 + e_4 \rangle = -(\gamma_2 + \mu)I_2 - \beta_2 S_2 I_2 < 0$ and

ii. if $S_2 = 0$, then $\langle f(q), e_2 \rangle = -\|f(q)\| < 0$.

(b) if $S_2 = 0$, then

i. if $I_2 + S_1 = N$, then $\langle f(q), e_2 + e_3 \rangle = -\|f(q)\| < 0$ and

ii. if $S_1 = 0$, then $\langle f(q), e_2 \rangle = -\|f(q)\| < 0$.

For the other components of $\partial\Omega_5$ the proofs are analogous.

So, given $q \in \Omega$ and $\phi(t,q)$ a solution that passes through q at $t = 0$, then $\phi(t,q)$ does not cross $\partial\Omega$. Hence, $\phi(t,q) \in \Omega$ for all $t \geq 0$ and for all $q \in \Omega$, that is, Ω is positively flow-invariant. □

Theorem 3.2. *A Lyapunov function for system* (3.2) *in* Ω *is*

$$L = I_1 + I_2 + S_1 + S_2.$$

Proof. Note that for $\mathbf{x} = (I_1, I_2, S_1, S_2) \in \Omega$, we have

$$\begin{aligned} L'(\mathbf{x}) &= I_1' + I_2' + S_1' + S_2' \\ &= -\gamma_1 I_1 - \lambda I_1 + \lambda I_1 - \gamma_2 I_2 - \mu I_2 \\ &= -\gamma_1 I_1 - \gamma_2 I_2 - \mu I_2 \\ &= -\gamma_1 I_1 - (\gamma_2 + \mu) I_2. \end{aligned}$$

So if $\mathbf{x} \in \Omega \setminus \Omega^*$, then $L'(\mathbf{x}) < 0$ and if $\mathbf{x}^* = (0,0,S_1,S_2) \in \Omega^*$, then we have $L'(\mathbf{x}) = 0$. Therefore, each equilibrium point $\mathbf{x}^*$ of system (3.2) is stable. □

Remark: Thus, the point $\mathbf{x}^*$ can be called a Disease Free Equilibrium (DFE), in accordance with [17].

3.2 The Basic Reproduction Number

We now seek to determine the threshold value, $\mathscr{R}_0$, of model (3.1), which was considered to study the stability of the DFE, in accordance with [17].

Consider $\mathbf{x} = (I_1, I_2, S_1, S_2)$ and write system (3.1) in the form

$$\mathbf{x}' = \mathscr{F}(\mathbf{x}) - \mathscr{V}(\mathbf{x})$$

with

$$\mathscr{F} = \begin{pmatrix} \beta_1 S_1 I_1 + \beta_2 S_2 I_2 \\ 0 \\ 0 \\ 0 \end{pmatrix} \text{ e } \mathscr{V} = \begin{pmatrix} \gamma_1 I_1 + \lambda I_1 \\ \gamma_2 I_2 + \mu I_2 - \lambda I_1 \\ \beta_1 S_1 I_1 \\ \beta_2 S_2 I_2 \end{pmatrix}$$

with the DFE being $\mathbf{x}^* = (0,0,S_1,S_2) \in \Omega$. So at the point $\mathbf{x}^*$ we get the Infection Matrix

$$\mathbb{F} = \begin{pmatrix} \beta_1 S_1 & \beta_2 S_2 \\ 0 & 0 \end{pmatrix}$$

and the Transmission Matrix

$$\mathbb{V} = \begin{pmatrix} \gamma_1 + \lambda & 0 \\ -\lambda & \gamma_2 + \mu \end{pmatrix}$$

and from these we obtain the Next Generation Matrix

$$\mathbb{F}\mathbb{V}^{-1} = \begin{pmatrix} \frac{\beta_1 S_1(\mu+\gamma_2)+\beta_2 S_2 \lambda}{(\gamma_1+\lambda)(\mu+\gamma_2)} & \frac{\beta_2 S_2}{\mu+\gamma_2} \\ 0 & 0 \end{pmatrix}.$$

The number of individuals infected by an infected individual at each instant of time t is given by the spectral radius of the Next Generation Matrix, that is,

$$\mathscr{R}(t) = \frac{\beta_1 S_1(t)}{\gamma_1 + \lambda} + \frac{\lambda}{\gamma_1 + \lambda} \frac{\beta_2 S_2(t)}{\mu + \gamma_2}, \tag{3.4}$$

for $t \geq 0$.

Note that for each instant t, the term $\frac{\beta_1 S_1}{\gamma_1+\lambda}$ is the average number of infected individuals who are not health professionals, the factor $\frac{\lambda}{\gamma_1+\lambda}$ is the probability that an infected individual without severe symptoms, in other words, who are not hospitalized, I_1, will survive and will develop severe symptoms, requiring hospitalization, and the factor $\frac{\beta_2 S_2}{\mu+\gamma_2}$ is the number of healthcare individuals who are infected by an individual with severe symptoms. Hence, $\mathscr{R}(t)$ gives the total number of new individuals who are infected by I_1 or by I_2 and which continuously depends on $S_1(t)$ and $S_2(t)$, $t \geq 0$. Thus, $\mathscr{R}(0) = \mathscr{R}_0$ is the Basic Reproduction Number. In addition, for $t > 0$, we have that $\mathscr{R}(t)$ is the Effective Reproduction Number.

Figure 2 shows the evolution of subpopulations over time for a hypothetical model according to system (2.2). It is noteworthy that the populations in this case are non-real, the parameters were obtained empirically and do not correspond to the real data, and the curves are presented in order to better understand the behavior of the subpopulations. Later, in section 4, curves obtained according to real data are presented, as well as the respective parameters.

4 SIMULATIONS

For the simulations of model (2.2), data referring to the city of Manaus were considered, in which the population was taken as being 2.2 million inhabitants, of which 23,176 are health professionals [4, 7, 14].

In all simulations, model (2.2) and the parameter values and initial conditions presented in Tables 1 and 2, respectively, were used. The data on confirmed and obtained cases caused by COVID-19 were extracted from the COVID-19 Manaus report, prepared by the Municipal Health Secretariat

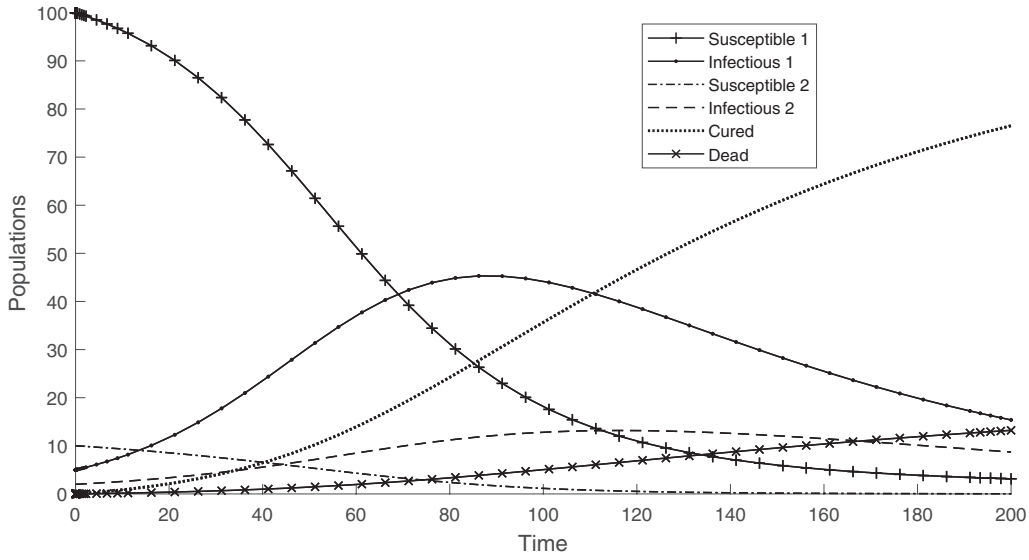

Figure 2: Solution curves of system (2.2). Made by the authors.

(SMS) of Manaus [16]. The simulations were carried out over a period of 155 days, which is equivalent to the period from March 31 to September 1, 2020, when there was the first wave of COVID-19 in Manaus, and a population unit corresponds to 10,000 individuals.

The simulations were made at software Octave, that have a set of solvers for initial value problems for Ordinary Differential Equations. In particular, we utilized the ode45 command, whose intern implementer is the Runge-Kutta method, a fourth–order accurate integrator therefore the local error normally expected is $O(h^5)$.

Table 1: Parameter values based on [12], except β_i, $i = 1,2$ which were obtained empirically.

β_1	β_2	γ_1	γ_2	μ	λ
0.00078	0.0009	0.0666	0.0500	0.0222	0.0250

Table 2: Initial conditions, according to [14, 16], with each population unit corresponding to 10,000 individuals.

$S_1(0)$	$S_2(0)$	$I_1(0)$	$I_2(0)$	$C(0)$	$M(0)$
217.6830	2.3176	0.1340	0.0134	0.0023	0.0002

In Figure 3, we present two curves: one that describes the evolution of the cumulative number of deaths caused by COVID-19 according to model (2.2) and another that represents the cumulative number of deaths caused by COVID-19 in the city of Manaus according to [16]. Note that these curves have similar profiles, indicating that the proposed model satisfactorily describes the

dynamics of COVID-19 in the city of Manaus, mainly between the 20th and the 100th day, but until the 100th day profiles are close, a period corresponding to that from March 31 to June 10, 2020.

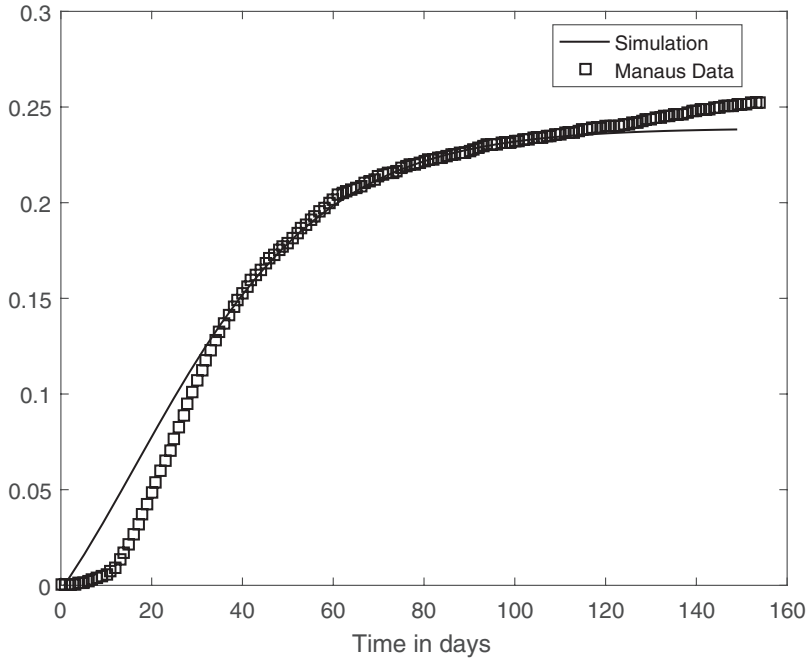

Figure 3: The line represents the cumulative number of deaths due to COVID-19 simulated according to model (2.2) and using the data in Tables 2 and 1. The irregular curve represents the cumulative number of deaths due to COVID-19 in Manaus, according to [16]. Made by the authors.

In Figure 4 we have: the evolution of the cumulative number of infected individuals, I, that is, those affected by COVID-19 over time according to the proposed model, with $I(t) = I_1(t) + I_2(t) + C(t) + M(t)$ and the evolution of the cumulative number of confirmed cases of COVID-19 in Manaus, according to [16]. These curves also have similar outlines during the first hundred days and, from the hundredth day onwards, the simulation curve (line curve) tends to stabilize, while the curve of cases confirmed by COVID-19 in Manaus is on the rise. Thus, through the model developed, it is possible to recommend that at the end of the hundredth day, the first wave of COVID-19 in the city of Manaus is over.

The basic reproduction number for the scenarios presented, using formula (3.4), at $t = 0$, is $\mathscr{R}_0 = 1.83$, indicating that at the beginning of the pandemic (March 31, 2020) each infectious individual, when exposed to the susceptible population, infected an average of 1.83 individuals, enough for the epidemic to establish itself, as can be seen by the number of confirmed cases over time in Manaus, see Figure 4. The curve of the effective reproduction number of model (2.2),

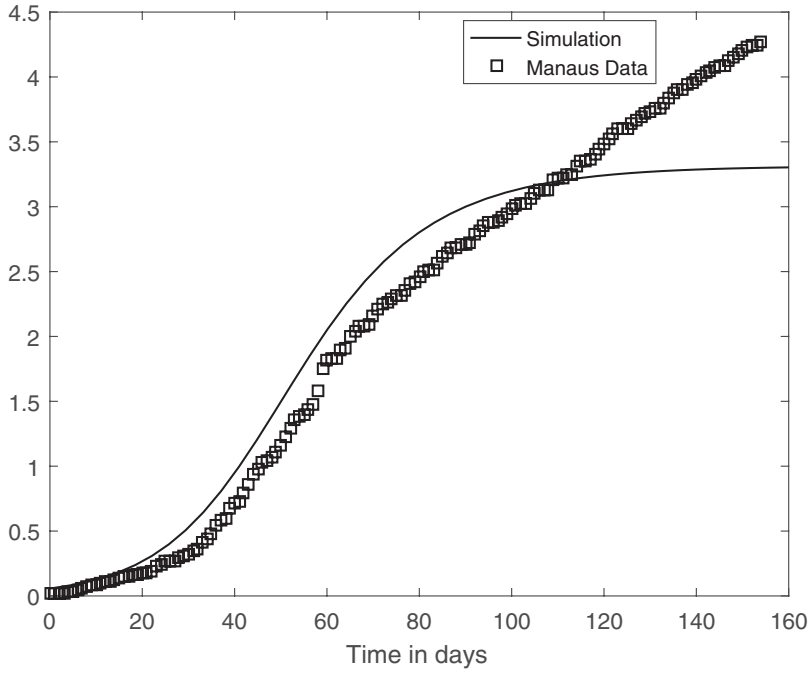

Figure 4: The line curve represents the cumulative number of people infected by COVID-19, $I = I_1 + I_2 + C + M$, obtained by simulating the model (2.2) with data from Tables 2 and 1; the irregular curve represents the cumulative number of confirmed cases of COVID-19 in Manaus, according to [16]. Made by the authors.

given by the function in (3.4) which represents the number of new individuals infected by I_1 and/or by I_2 at each instant of time is shown in Figure 5; the simulation period here is greater than 155 days in order to have a better visualization of the profile of this curve. Also, from the curve in Figure 5, the total number of new individuals infected by COVID-19 is decreasing over time, and on the hundredth day (June 10, 2020) this number is already lower than 1, indicating that the transmission of the disease is slowing down, corroborating the stability of the simulated curve of those infected by COVID-19, see Figure 4. In Figure 6 (b), the effective reproduction number obtained from the seven-day moving average of the number of confirmed daily cases of COVID-19 in the city of Manaus is shown, according to [16]. Comparing Figures 5, 6 (a) and 6 (b) it is possible to notice that, in fact, there is a drop in the values of R_t right after the beginning of the epidemic in Manaus until it reached stability. The oscillations in R_t in Figure 6 (b) can be justified by the exposure of the susceptibles who were in isolation, which is not foreseen in model (2.2). Furthermore, due to the emergence of new variants of the virus, among other possibilities, there is a variation in the strength of infection, that is also reflected in the value of R_t, which was already expected.

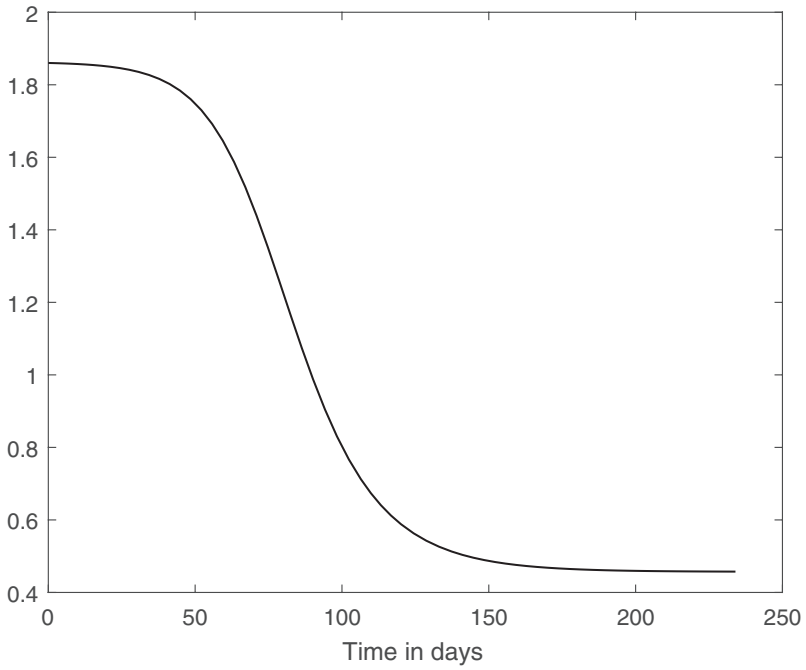

Figure 5: Effective reproduction number described by the function (3.4) with data from Tables 1 and 2 and simulated data from (2.2). Made by the authors.

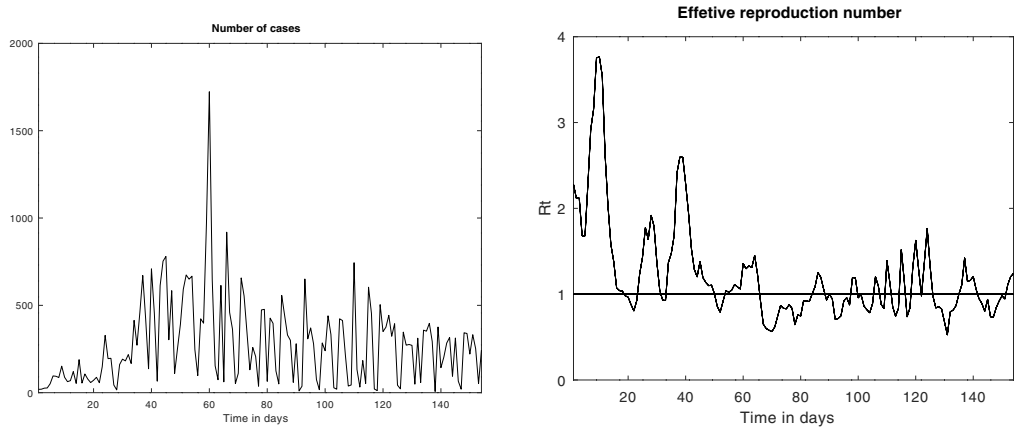

(a) Number of daily cases of COVID-19.

(b) Effective number.

Figure 6: Data from COVID-19 for the period from March 31 to September 1, 2020, in Manaus, according to [16]. Made by the authors.

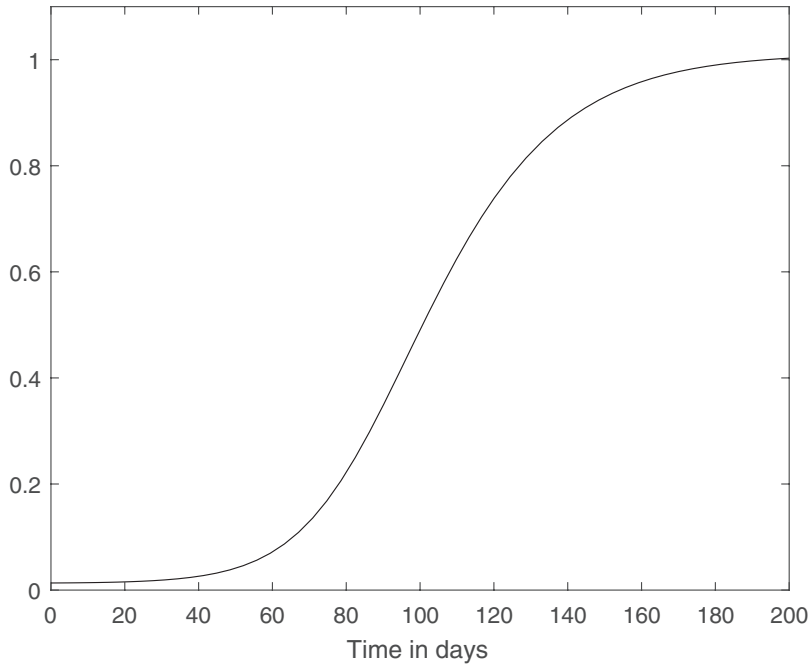

Figure 7: Health professionals infected according to model (2.2) and data from Tables 1 and 2. Made by the authors.

According to the Amazonas State Department of Health (SES-AM), among those health professionals in Manaus who were tested for COVID-19 in April 2020, the percentage of positives was 29%, in early May 2020 this percentage dropped to around 5.5%, but in July it reached 10% [14, 15]. SES-AM and the Manaus SMS did not disclose the numbers of healthcare professionals infected over time, but according to our model we had $4,903$ healthcare professionals infected with SARS-CoV-2 in Manaus by the 100th day, which constitutes 21.15% of professionals. In Figure 7 we present the profile of the curve of healthcare professionals infected over time according to model (2.2).

We emphasize that the parameter values were obtained considering the total population of Manaus as being susceptible. However, if we assume that the portion of the population in isolation is 40%, for example, new simulations must be carried out to determine the parameters for this scenario.

5 FINAL CONSIDERATIONS

The model proposed in this article contemplates a different dynamic from those of classic epidemiological models regarding the process of contamination by COVID-19, since it considers a greater susceptibility for health professionals, as they are in direct contact with patients who

are hospitalized and infected with the virus. In this way, the modeling encompasses a COVID-19 contagion dynamic that makes this mathematical model closer to reality.

Through a qualitative analysis, it was verified that the biological space of the model is positively invariant by flow, a necessary condition for the validation of an epidemiological model. In addition, the basic reproduction number, which indicates the total number of new individuals that are infected over time, was also determined, and this number depends continuously on the number of susceptible individuals S_1 and S_2.

The solution curves of the model for the number of infected and number of deaths, obtained from the simulations, present profiles similar to the curves of confirmed cases and deaths by COVID-19 in the city of Manaus, showing the validity of the model in the period of the first wave in this city, with $\mathscr{R}_0$ being estimated to be 1.83 and with an estimated $4,903$ healthcare professionals infected by the 100th day, as of March 31, 2020.

Finally, it is noteworthy that the emergence of other waves can be justified by the exposure of susceptible individuals who were in isolation and/or by the development of new variants of the virus, which alters the infectiousness of the disease. However, if the quarantine that started in March had been maintained, the results would be in accordance with what was presented.

Acknowledgments

Author L. T. Takahashi had partial support from Coordenação de Aperfeiçoamento de Pessoal de Nível Superior - Brasil (CAPES) - Financing Code 001.

REFERENCES

[1] V. Capasso. “Mathematical structures of epidemic systems”, volume 88. Springer (1993).

[2] I. Cooper, A. Mondal & C.G. Antonopoulos. A SIR model assumption for the spread of COVID-19 in different communities. *Chaos, Solitons & Fractals*, **139** (2020), 110057.

[3] L. Edelstein-Keshet. “Mathematical Models in Biology”. Society for Industrial and Applied Mathematics, Vancouver, BC, Canada (2005).

[4] G1 AM. Em Manaus, 62,8 mil trabalhadores da saúde foram vacinados contra Covid-19 (2021). URL: https://g1.globo.com/am/amazonas/noticia/2021/03/19/em-manaus-628-mil-trabalhadores-da-saude-foram-vacinados-contra-covid-19.ghtml Accessed on: 05/03/2021.

[5] G. Gaeta. A simple SIR model with a large set of asymptomatic infectives. *Mathematics in Engineering*, **3**(2) (2021), 1–39.

[6] Y.R. Guo, Q.D. Cao, Z.S. Hong, Y.Y. Tan, S.D. Chen, H.J. Jin, K.S. Tan, D.Y. Wang & Y. Yan. The origin, transmission and clinical therapies on coronavirus disease 2019 (COVID-19) outbreak – An update on the status. *Military Medical Research*, **7**(1) (2020), 1–10.

[7] Instituto Brasileiro de Geografia e Estatística. Brazil/Amazonas/Manaus (2020). URL: https://cidades.ibge.gov.br/brasil/am/manaus/panorama Accessed on: 05/03/2021.

[8] W.O. Kermack & A.G. McKendrick. A contribution to the mathematical theory of epidemics. *Proceedings of the royal society of london. Series A, Containing papers of a mathematical and physical character*, **115**(772) (1927), 700–721.

[9] Ministério da Saúde. Primeiro caso de Covid-19 no Brasil permanece sendo o de 26 de fevereiro (2020). URL: https://www.gov.br/saude/pt-br/assuntos/noticias/primeiro-caso-de-covid-19-no-brasil-permanece-sendo-o-de-26-de-fevereiro Accessed on: 09/28/2020.

[10] R. Mukherjee, A. Kundu, I. Mukherjee, D. Gupta, P. Tiwari, A. Khanna & M. Shorfuzzaman. IoT-cloud based healthcare model for COVID-19 detection: an enhanced k-Nearest Neighbour classifier based approach. *Computing*, (2021), 1–21.

[11] K.N. Nabi. Forecasting COVID-19 pandemic: A data-driven analysis. *Chaos, Solitons & Fractals*, **139** (2020), 110046.

[12] Organização Pan-Americana da Saúde. Folha informativa COVID-19 – Escritório da OPAS e da OMS no Brasil (2020). URL: https://www.paho.org/pt/covid19 Accessed on: 09/28/2020.

[13] D. Ray, M. Salvatore, R. Bhattacharyya, L. Wang, J. Du, S. Mohammed, S. Purkayastha, A. Halder, A. Rix, D. Barker, M. Kleinsasser, Y. Zhou, D. Bose, P. Song, M. Banerjee, V. Baladandayuthapani, P. Ghosh & B. Mukherjee. Predictions, role of interventions and effects of a historic national lockdown in India's response to the COVID-19 pandemic: data science call to arms. *HHS Public Access*, (2020).

[14] Secretaria de Estado de Saúde - Governo do Estado do Amazonas. Notícias (2020). URL: http://www.saude.am.gov.br/visualizar-noticia.php?id=4518 Accessed on: 06/15/2021.

[15] Secretaria de Estado de Saúde - Governo do Estado do Amazonas. Notícias (2020). URL: http://www.saude.am.gov.br/visualizar-noticia.php?id=4849 Accessed on: 06/15/2021.

[16] Secretaria Municipal de Saúde - Prefeitura de Manaus. Relatório Covid-19 Manaus (2021). URL: https://covid19.manaus.am.gov.br/wp-content/uploads/Relatório-Covid-v2.0-07_08_09_05-2021.pdf Accessed on: 05/03/2021.

[17] P. Van Den Driessche & J. Watmough. Reproduction numbers and sub-threshold endemic equilibria for compartmental models of disease transmission. *Mathematical Biosciences*, **180**(1-2) (2002), 29–48.

[18] World Health Organization. Brazil Situation (2020). URL: https://covid19.who.int/region/amro/country/br Accessed on: 09/28/2020.